

THERMAL AND STRESS ANALYSIS OF AN X-RAY TARGET FOR 6 MEV MEDICAL LINEAR ACCELERATORS*

Zhihui Wang^{1,2*}, Hao Zha^{1,2}, Jiaru Shi^{1,2†}, Huaibi Chen^{1,2}

¹ Department of Engineering Physics, Tsinghua University, Beijing 100084, CHN

² Key Laboratory of Particle & Radiation Imaging of Ministry of Education, Tsinghua University, Beijing 100084, CHN

Abstract

We present an optimal design of an X-ray target for 6 MeV medical linear accelerators using FLUKA simulations. The target is composed of high-atomic-number material (tungsten) and high-thermal-conductivity material (copper). For 6 MeV electron beam with 100 μ A current, the results show that the target can achieve 1014 cGy/min at 1 meter in front of the target. Furthermore, we analyse the temperature and thermal stress responses of the target under transient thermal loads using Ansys Code. Within 100 ms, the maximum temperature reaches 512 $^{\circ}$ C under pulsed heating source with 250 Hz frequency and 1% duty cycle and the number of cycles to failure is estimated as 5.8e8, which corresponds to 644-hour operation.

INTRODUCTION

Medical linear accelerators are the most commonly used device for external beam radiation treatments for patients with cancer [1]. The X-ray target is a very important component at the end of the accelerating tube to produce high-energy X-ray. The incident electron beam hits the metal target to produce high-energy photons through bremsstrahlung, then the X-ray passes through the collimators and flattening filter to produce uniform and stable X-ray beam [2].

Targets of different materials and different thicknesses have different conversion efficiency. Monte-Carlo Method is the most popular tool to calculate the yield of the X-ray and optimize the design of the target [3]. At the same time, when the electron beam hits the target, large amounts of heat deposit within the target, which may cause the melt of the target. Besides, high-intensity and high-frequency pulsed heating source produces thermal cycles and stress, causing thermal fatigue, which may lead to degradation of target's structural integrity and reduction of its lifetime. There are three stages of metal fatigue: crack initiation in the areas of stress concentration, incremental crack propagation, final catastrophic failure [4]. The ductile-brittle transition temperature, or DBTT for tungsten is comparatively high, 250 $^{\circ}$ C for hot rolled tungsten and 350 $^{\circ}$ C for hot forged tungsten, which are close to the working temperature of the X-ray target [5]. As the temperature cycle crosses the DBTT frequently, tungsten target shifts between flexible and brittle, easily initiating cracking. Finite element analysing software, Ansys workbench is often used to simulate the thermal and stress performance of X-ray targets [6].

Previous studies on thermal stability of X-ray targets concentrate on steady state temperature distribution, few knowledge has been obtained about the transient thermal and structural performances. This study presents a tungsten-copper composite target and calculates the energy deposition distribution of the target, revealing the transient thermal and stress responses.

MODEL

The transverse intensity distribution of incident electron beam is assumed as Gaussian distribution with FWHM of 0.6 mm. The energy spectrum of electron source is generated by a 6 MeV accelerating tube which is designed by Jiahang Shao in department of engineering physics, Tsing-hua [7]. The beam current is set as 100 μ A. The repetition frequency and duty cycle are set as 250 Hz and 1%, re-spectively. Figure 1 shows the temporal distribution of the pulsed power source.

Model for FLUKA Simulations

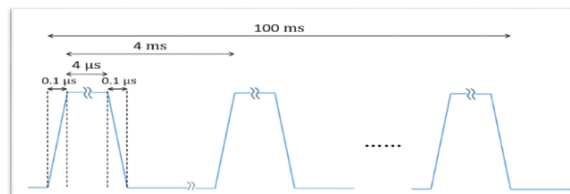


Figure 1: Temporal distribution of power sources.

We choose tungsten as the first layer of the target for higher photon yield, copper as the second layer for better heat dissipation effect. Figure 2 shows a cross section of the model used in FLUKA simulations for optimization of the target and calculation of energy deposition profile in the target. The target is divided into 98 parts; energy deposition is recorded individually. A photon dose rate detector is set at 1m distance to the position the electron beam hits the target, an area detector is set at the bottom of copper to record electrons leakage.

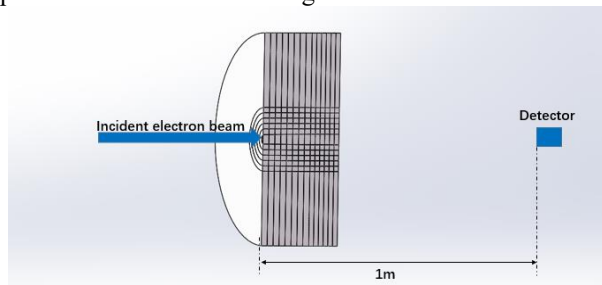


Figure 2: Model for FLUKA simulations.

Content from this work may be used under the terms of the CC BY 3.0 licence (© 2018). Any distribution of this work must maintain attribution to the author(s), title of the work, publisher, and DOI.

* zhihui-w16@mails.tsinghua.edu.cn

† shij@mail.tsinghua.edu.cn

Model for Ansys Code

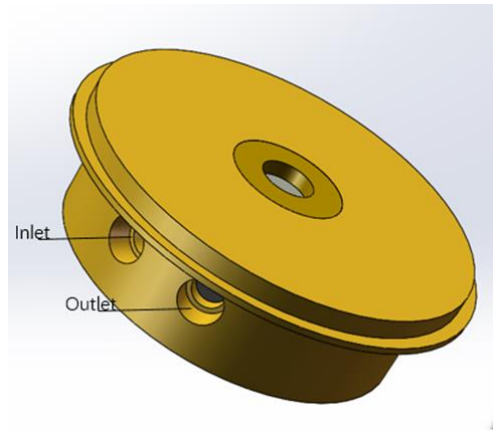


Figure 3: Overview of target with cooling system.

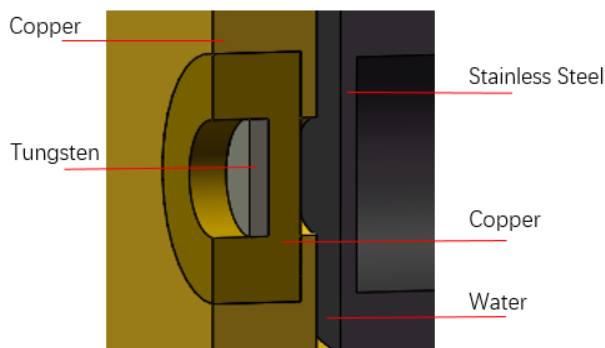


Figure 4: Profile of target with cooling system.

Table 1: Properties of Materials in Ansys Code

Properties	Tungsten	Copper	Stainless Steel
Density(kg/m ³)	19300	8933	7872
Coefficient of Thermal Expansion(°C ⁻¹)	4.5e-6	1.75e-5	1.2e-5
Young's Modulus(Pa)	3.447e11	1.06e11	1.9e11
Poisson's Ratio	0.28	0.324	0.305
Isotropic Thermal Conductivity(W/m*°C)	174	400	45
Specific Heat(J/kg*°C)	132	385	481
Melting point(°C)	3410	1083	1500

Figure 3 shows a conceptual design of the target with the cooling system. Figure 4 shows the profile of the target with the cooling system. Table 1 shows the properties of the materials used in Ansys code. The energy deposition profile is transferred into Ansys workbench simulation for analysis of thermal and stress performance. The inlet temperature and velocity are set as 20 °C and 5 L/min, respectively. The initial temperature is set at room temperature 22 °C. A uniform velocity profile is assumed. The outlet pressure is set at one bar pressure. Air convection heat transfer coefficient is set as 5 W/(m²*°C). For simplification, the target is assumed to be fixed by the surrounding structure.

RESULTS

Optimization of the Target

FLUKA simulations are used to scan the thickness of tungsten and copper to find the thickness combination with the largest photon dose rate. Considering that the electron energy leakage percentage must be below 1%, we choose the proper composite target with 1.2 mm tungsten and 2 mm copper. Figure 5 shows the dose rate distribution of composite targets. As Fig. 6 shows, the dose rate is 1014 cGy/min/100 μA, the electron energy leakage percentage is 0.24%.

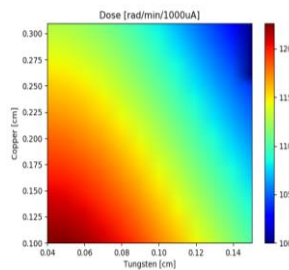


Figure 5: Dose rate of composite targets.

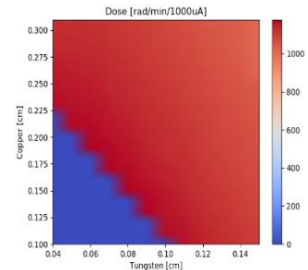


Figure 6: Dose rate of composite targets with leak energy.

Calculation of Target Energy Deposition Distribution

The target is divided into 98 parts altogether radially and longitudinally. Heating power density distributions of incident electron beam with different transverse intensity distribution are compared. Outcomes of Gaussian transverse intensity distributions with FWHM of 0.4 mm, 0.6 mm and 0.8 mm are showed in Fig. 7, Fig. 8 and Fig. 9, respectively. The more concentrated is the transverse intensity distribution, the more concentrated is the heating power density distribution. For transverse intensity distribution with 0.6mm FWHM, the maximum body heating power is 1.86e15 W/m³, located at 0.2 mm-0.4 mm to the top of tungsten target.

Transient Thermal and Stress Analysis

Transverse intensity Gaussian distribution with 0.6 mm FWHM is adopted. The maximum steady state temperature distribution of the vertical cross section of the target within 100 ms locally is showed in Fig. 10. The peak temperature altogether is 512 °C located at the point 0.3 mm to the top of tungsten target. The peak temperature in copper is 145 °C, located at the border of tungsten and copper. The maximum transient temperature variation curve of tungsten and copper within 100 ms are given by Fig. 11 and Fig. 12, respectively. The maximum Von-Mises strain and Von-Mises stress distribution of the target within one single pulse are presented in Fig. 13 and Fig. 14 respectively.

Content from this work may be used under the terms of the CC BY 3.0 licence (© 2018). Any distribution of this work must maintain attribution to the author(s), title of the work, publisher, and DOI.

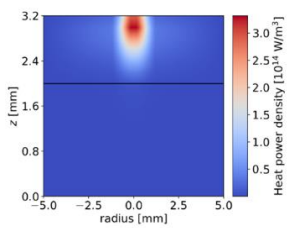


Figure 7: Heat power density of 0.4 mm FWHM transverse distribution.

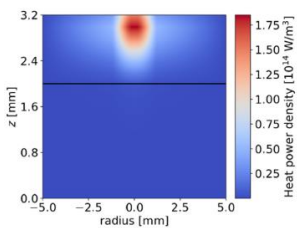


Figure 8: Heat power density of 0.6 mm FWHM transverse distribution.

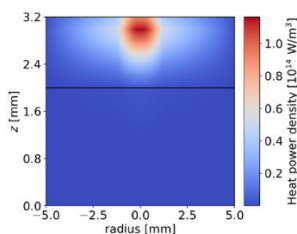


Figure 9: Heat power density of 0.8 mm FWHM transverse distribution.

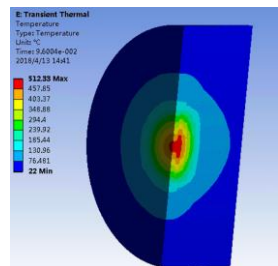


Figure 10: Maximum temperature distribution within 100 ms.

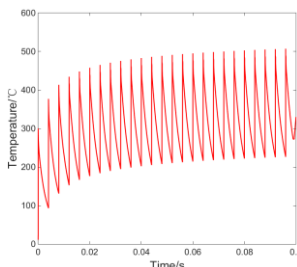


Figure 11: Tungsten temperature variation within 100 ms.

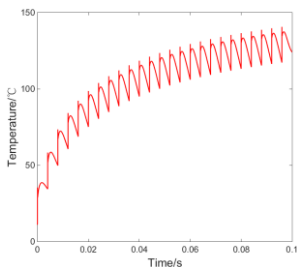


Figure 12: Copper temperature variation within 100 ms.

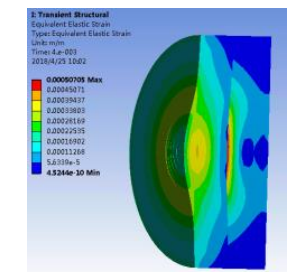


Figure 13: Maximum Von-Mises strain distribution within one pulse.

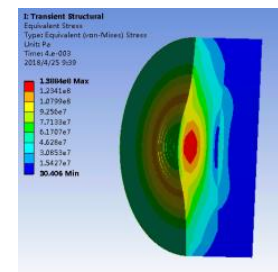


Figure 14: Maximum Von-Mises stress distribution within one pulse.

Thermal Fatigue Analysis

Since the target is restrained, thermal cycles cause expansion and contraction, hence generating thermal stress [4-5]. According to the material fatigue theory, the

Basquin equation used to describe the relationship between stress amplitude and the number of cycles to failure for the high cycle, low strain regime is expressed as:

$$S_a = S_f' (2N_f)^b \quad (1)$$

Where S_f' and b are fatigue strength coefficient and exponent, respectively. N_f represents number of cycles to failure. Jemila Habainy et al. did experiments on relationship between number of cycles to failure and stress amplitude of sintered and HIPed tungsten, presenting the conservative relationship through regression analysis [8]:

$$S_a = 376.94 \times (2N_f)^{-0.0501} \quad (2)$$

In this study, for 6 MeV incident electron beam with 100 μ A beam current, steady state stress amplitude is estimated as 132.5 MPa, the estimated number of cycles to failure is 5.8e8, which corresponds to 644 h operation with 250 Hz frequency and 1% duty cycle.

CONCLUSION

The target can deliver 1014 rad/min/100 μ A at 1 meter in front of the target. The target won't melt and number of cycles to failure is estimated as 5.8e8. More properties of thermal fatigue of the target require further experiments.

REFERENCE

- [1] Qiang Gao and Hao Zha, "Design and optimization of the target on electron linear accelerator", in Proc. IPAC'13, Shanghai, China, May 2013, paper THPWA016, pp. 3663-3665.
- [2] Ajaj, F. A. A., and N. M. H. Ghassal. "An MCNP-based model of a medical linear accelerator X-ray photon beam", *Australasian Physics & Engineering Sciences in Medicine*, vol. 26, no. 3, pp. 140-144, 2003.
- [3] Shi, Yinghua, et al. "Monte Carlo simulation of 6 MV medical electron linear accelerator", *Chinese Journal of Radiological Medicine and Protection*, vol. 31, no.3, pp. 220-224, 2011.
- [4] David P. Pritzkau, "RF Pulsed Heating", Ph.D. thesis, Stanford Linear Accelerator Centre, Stanford, CA 94309, 2001.
- [5] Shen, Tielong, Yong Dai, et al. "Microstructure and tensile properties of tungsten at elevated temperatures", *Journal of Nuclear Materials*, vol. 468, pp. 348-354, 2016.
- [6] Jin, Ming, et al. "Thermal and stress analysis of window target or accelerator-driven sub-critical system during beam trip transients", *Progress in Nuclear Energy*. vol. 85, pp. 325-332, 2015.
- [7] Jiahang Shao and Hao Zha, "High power test of a C-Band 6MeV standing-wave linear accelerator", in Proc. IPAC'13, Shanghai, China, May 2013, paper THPWA018, pp. 3666-3668.
- [8] Jemila Habainy et al. "Fatigue properties of tungsten from two different processing routes", *Journal of Nuclear Materials* pp. 1-9, 2017.